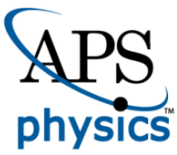

Active Phase Separation in Mixtures of Chemically Interacting Particles

Jaime Agudo-Canalejo and Ramin Golestanian

Phys. Rev. Lett. **123**, 018101 — Published 3 July 2019

DOI: 10.1103/PhysRevLett.123.018101

Active phase separation in mixtures of chemically-interacting particles

Jaime Agudo-Canalejo[1, 2, *] and Ramin Golestanian[3, 1, †]

[1] *Rudolf Peierls Centre for Theoretical Physics, University of Oxford, Oxford OX1 3PU, United Kingdom*
[2] *Department of Chemistry, The Pennsylvania State University, University Park, Pennsylvania 16802, USA*
[3] *Max Planck Institute for Dynamics and Self-Organization (MPIDS), D-37077 Göttingen, Germany*

(Dated: May 20, 2019)

We theoretically study mixtures of chemically-interacting particles, which produce or consume a chemical to which they are attracted or repelled, in the most general case of many coexisting species. We find a new class of active phase separation phenomena in which the nonequilibrium chemical interactions between particles, which break action-reaction symmetry, can lead to separation into phases with distinct density and stoichiometry. Due to the generic nature of our minimal model, our results shed light on the underlying fundamental principles behind nonequilibrium self-organization of cells and bacteria, catalytic enzymes, or phoretic colloids.

Microorganisms and cells can chemotax in response to gradients of chemicals that they themselves produce or consume [1, 2]. The same behaviour has been recently observed at the nanoscale for individual enzymes [3–5], and can be mimicked in synthetic systems using catalytically-active phoretic colloids [6–13] . Importantly, when many such particles are placed in solution, they interact with each other through their influence on the chemical's concentration field. Chemical interactions underlie a wide variety of phenomena such as self-organisation in heterogeneous populations of microorganisms and cells (e.g. quorum sensing [14] and competition for nutrients [15] in bacterial ecosystems, or cell-cell communication *via* chemokines [16]); aggregation of enzymes that participate in common catalytic pathways into a metabolon [17–19], which could be harnessed in the design of better synthetic pathways [20]; or the self-assembly of active materials from catalytic colloids [21, 22].

A key feature of chemical interactions between two different species—whether they are synthetic catalytic colloids, biological enzymes, or whole cells or microorganisms—is that they are in general non-reciprocal [7, 8]. The concentration field of a fast-diffusing chemical around a chemically-active particle of species i is, to lowest order, given by $c - c_0 \propto \alpha_i / r$ where α_i is the activity of the species (positive and negative for producer and consumer species), r is the distance to the particle's centre, and c_0 is the reference concentration of the chemical at infinity. In turn, the motion of a particle of species j in response to gradients of the chemical is given by a velocity $\boldsymbol{V}_j = -\mu_j \nabla c$ where μ_j is the mobility of the species (positive or negative if the species is directed towards regions of lower or higher concentration of the chemical). Combining these two expressions, one finds that the velocity of the j-species particle in response to the presence of the i-species particle is $\boldsymbol{V}_{ij} \propto \alpha_i \mu_j \boldsymbol{r}_{ij} / |\boldsymbol{r}_{ij}|^3$ with $\boldsymbol{r}_{ij} = \boldsymbol{r}_j - \boldsymbol{r}_i$, whereas the velocity of the latter in response to the presence of the former is $\boldsymbol{V}_{ji} \propto -\alpha_j \mu_i \boldsymbol{r}_{ij} / |\boldsymbol{r}_{ij}|^3$. Note that in general $\boldsymbol{V}_{ij} \neq -\boldsymbol{V}_{ji}$ for $i \neq j$ because $\alpha_i \mu_j \neq \alpha_j \mu_i$, implying a broken action-reaction symmetry for inter-species interactions, which would be impossible in a system at thermodynamic equilibrium [23].

We have performed Brownian dynamics simulations [24] of the model just described for a wide range of mixtures of chemically-interacting species; see Fig. 1 and movies 1–12 in the Supplemental Material [24]. For binary mixtures we find that, while in a large region of the parameter space the mixtures remain homogeneous, the homogeneous state can also become unstable leading to a great variety of phase separation phenomena. Here, phase separation is used in the sense of macroscopic (system-spanning) separation typically into a single large cluster (occasionally into two; see Fig. 1(a)) that coexists with a dilute (or empty) phase. The phase separation process may lead to aggregation of the two species into a single mixed cluster, or to separation of the two into either two distinct clusters or into a cluster of a given stoichiometry and a dilute phase. The resulting configurations are qualitatively distinct for mixtures of one chemical-producer and one chemical-consumer species, as opposed to mixtures of two producer (or consumer) species; compare panels (a) and (c) in Fig. 1. While the typical steady-state configurations are static, for mixtures of producer and consumer species we also find that static clusters can undergo a shape-instability that breaks their symmetry, leading to a self-propelling macrocluster (Fig. 1(b), movies 8 and 9). Randomly-generated highly-polydisperse mixtures of up to 20 species also show homogeneous as well as phase-separated states (Fig. 1(d), movies 11 and 12).

In the following, we will show how these results can be understood by means of a continuum theory, and how the observed phase separation behaviour is intimately related to the non-equilibrium and non-reciprocal character of the interactions. This represents a fundamentally new class of active phase separation, in which the activity arises from the non-equilibrium nature of the interactions between particles that are otherwise non-motile, rather than from the intrinsic activity of self-propelling particles as commonly studied [25–36].

We consider a system consisting of M different species

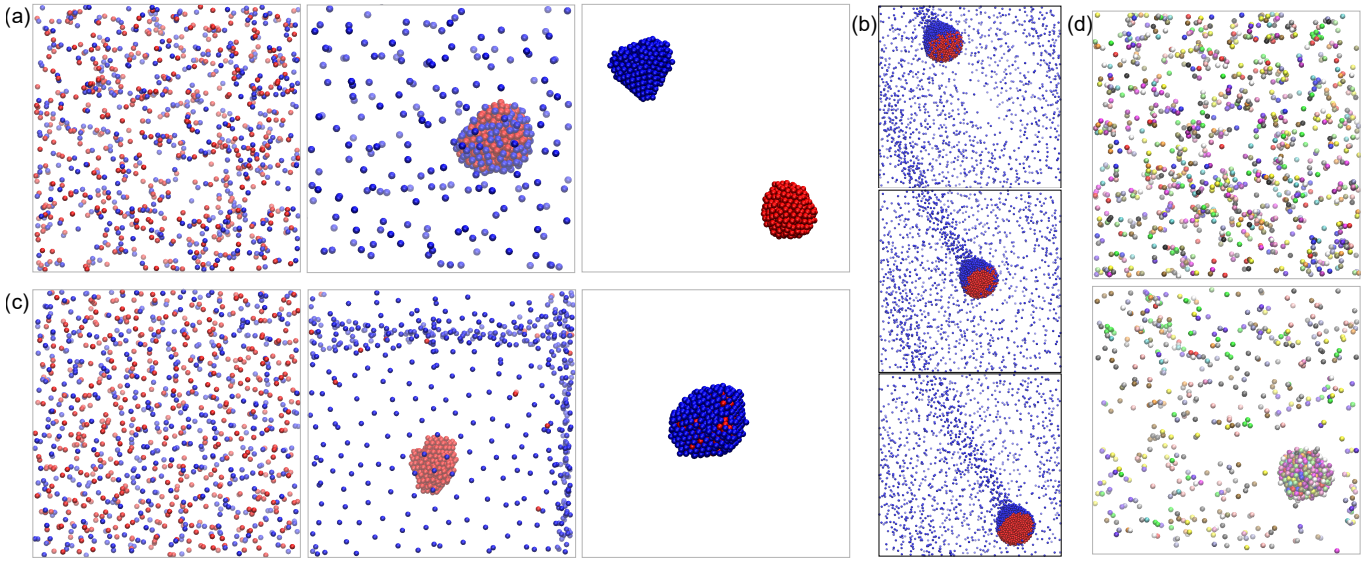

FIG. 1. Mixtures of chemically-interacting particles display a wealth of active phase separation phenomena. (a) Binary mixtures of producer (red) and consumer (blue) species show, from left to right, homogeneous states with association of particles into small "molecules", aggregation into a static dense phase that coexists with a dilute phase, and separation into two static collapsed clusters; see movies 1–3 in the Supplemental Material [24]. (b) The static aggregate (a, centre) can undergo symmetry breaking to form a self propelled macroscopic cluster; see movies 8 and 9. (c) Binary mixtures of producer species (red and blue) show homogeneous states without molecule formation, separation into a static dense phase and a dilute phase that is depleted near the dense phase, and aggregation into a static collapsed cluster; see movies 4–6. (d) Randomly-generated highly polydisperse mixtures (20 different species) can remain homogeneous or undergo macroscopic phase separation; see movies 11 and 12. Simulation parameters for each case (a–c) can be found in the description of the corresponding movies.

of chemically-interacting particles, with concentrations $\rho_i(\boldsymbol{r},t)$ for $i = 1, ..., M$; and a messenger chemical with concentration $c(\boldsymbol{r},t)$. The concentration of species i is described by $\partial_t\rho_i(\boldsymbol{r},t) - \nabla\cdot[D_\mathrm{p}\nabla\rho_i + (\mu_i\nabla c)\rho_i] = 0$ which includes a diffusive term with diffusion coefficient D_p, which for simplicity is taken to be equal for all species (implying that all particles are of similar size or, in the case of microorganisms, all species show a similar baseline level of non-directed random motion); as well as an advective term describing motion in response to gradients of the chemical. The concentration of the chemical is described by $\partial_t c(\boldsymbol{r},t) - D\nabla^2 c = \sum_i \alpha_i\rho_i$ which includes diffusion with coefficient D, and production or consumption of the chemical by all particle species. Performing a linear stability analysis [24] of this coupled system of $M+1$ equations around a spatially-homogeneous state with particle densities $\rho_i(\boldsymbol{r},t) = \rho_{0i}$, in the limit of a fast-diffusing chemical, we find that the homogeneous state becomes unstable towards a spatially-inhomogeneous state when the following condition holds

$$\sum_i \mu_i\alpha_i\rho_{0i} < 0. \qquad (1)$$

The instability corresponds to macroscopic phase separation, in the sense that it occurs for perturbations of infinite wave length, specifically for perturbations with wave number $\boldsymbol{q}^2 < -(DD_\mathrm{p})^{-1}\sum_i \mu_i\alpha_i\rho_{0i}$, with those having infinite wave length $\boldsymbol{q}\to 0$ being the first and most unstable. Importantly, the stability analysis also tells us about the stoichiometry of the different particle species at the onset of growth of the perturbation, which follows

$$(\delta\rho_1, \delta\rho_2, ..., \delta\rho_M) = \left(1, \frac{\mu_2\rho_{02}}{\mu_1\rho_{01}}, ..., \frac{\mu_M\rho_{0M}}{\mu_1\rho_{01}}\right)\delta\rho_1. \qquad (2)$$

If only a single particle species is present ($M = 1$), the instability criterion (1) describes the well-known Keller-Segel instability [37], which simply says that the homogeneous state is stable for particles that repel each other ($\mu_1\alpha_1 > 0$), whereas particles that attract each other ($\mu_1\alpha_1 < 0$) tend to aggregate, with the end state being a featureless macroscopic cluster containing all particles. In contrast, we will now show that as soon as we have mixtures of more than one species, the combination of the instability criterion (1) and the stoichiometric relation (2) predicts a wealth of new phase separation phenomena.

For binary mixtures ($M = 2$), the instability condition (1) becomes $\mu_1\alpha_1\rho_{01} + \mu_2\alpha_2\rho_{02} < 0$, and the stoichiometric constraint (2) implies that when μ_1 and μ_2 have equal or opposite sign, the instability will lead respectively to aggregation or separation of the two species. Combining these criteria we can construct a stability diagram for the binary mixture, although we must distinguish between two qualitatively-different kinds of mixtures: those of one

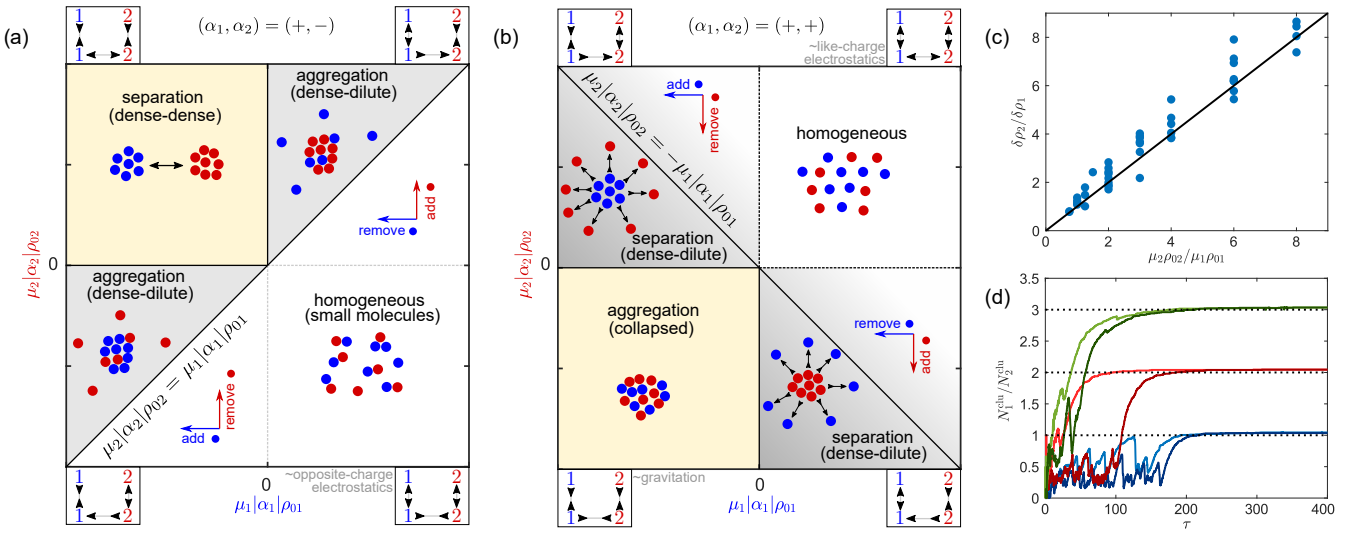

FIG. 2. (a) Stability diagram for mixtures of one producer and one consumer species (cf. Fig. 1(a)), and (b) for mixtures of two producer species (cf. Fig. 1(c)). In (a,b) the boxed legends attached to each quadrant symbolise the "interaction network" representing the sign of interactions between each species in the system, as described in the main text. Phase separation (aggregation in (a), separation in (b)) can be triggered by addition or removal of particles (density changes) only when interactions between the two species are intrinsically non-reciprocal. (c) Stoichiometry at the onset of the instability, obtained from 44 simulations (blue circles, see Table S1 in the Supplemental Material [24]) compared to the stability analysis prediction (Eq. 2). (d) Time evolution of the stoichiometry of the biggest cluster arising from aggregation of $(\alpha_1, \alpha_2) = (+, -)$ mixtures, demonstrating that the long time stoichiometry is predicted by the neutrality rule (Eq. 3) and is independent of the species' mobility (blue: $\tilde{\alpha}_2 = -1$, $\tilde{\mu}_2 = 8$ and 12; red: $\tilde{\alpha}_2 = -2$, $\tilde{\mu}_2 = 4$ and 8; green: $\tilde{\alpha}_2 = -3$, $\tilde{\mu}_2 = 3$ and 5; in all cases $N_1 = 800$, $N_2 = 200$, $\tilde{\alpha}_1 = \tilde{\mu}_1 = 1$).

producer and one consumer species, see Fig 2(a) where we have chosen $(\alpha_1, \alpha_2) = (+, -)$ without loss of generality; and those of two producer species, see Fig 2(b). The case of two consumer species is related to the latter by the symmetry $(\mu_1, \mu_2) \to -(\mu_1, \mu_2)$; see Fig. S1 in the Supplemental Material [24]. In this way, the parameter space for each type of mixture can be divided into regions leading to homogeneous, aggregated, or separated states, which correspond directly to those observed in simulations; compare Fig 2(a,b) to Fig. 1(a,c). We note, however, that while for $(\alpha_1, \alpha_2) = (+, -)$ mixtures the simulations are always seen to match the predicted phase behaviour, for $(\alpha_1, \alpha_2) = (+, +)$ mixtures we have observed separation even when the continuum theory predicts the homogeneous state to be linearly stable, although proceeding much more slowly (see movie 7 in the Supplemental Material [24]), indicating that in this region separation may be occurring through a nucleation-and-growth process controlled by fluctuations. This is denoted as the shaded gray region extending past the instability line in Fig 2(b).

The wide variety of phase separation phenomena arising in these mixtures is intimately related to the active, non-reciprocal character of the chemical interactions. In particular, it is useful to consider the sign of both inter-species as well as intra-species interactions (as described above, species i is attracted to or repelled from species j when $\mu_i\alpha_j$ is negative or positive, respectively). In the stability diagrams in Fig. 2(a,b), we find that each quadrant corresponds to a distinct "interaction network" between species, as depicted in the boxed legends attached to every quadrant (as an example, the top-right interaction network in (a) can be read as "1 is attracted to 2, 2 is repelled from 1, 1 is repelled from 1, and 2 is attracted to 2"). We find that only three regions in the parameter space have passive analogs: (i) The bottom-right of (a) corresponds to electrostatics with opposite charges, where equals repel and opposites attract, allowing for the formation of small active molecules as studied in Refs. 7 and 8. (ii) The top-right of (b) corresponds to electrostatics with like charges, where all interactions are repulsive leading to a homogeneous state. (iii) The bottom-left of (b) corresponds to gravitation, where all interactions are attractive. The top-left of (a) can be thought of as the opposite of electrostatics (or as gravitation including a negative mass species), where equals attract and opposites repel. The remaining four quadrants involve intrinsically non-reciprocal interactions where one species chases after the other: in (a), a self-repelling species chases after a self-attracting species; whereas in (b), a self-attracting species chases after a self-repelling species. Importantly, we observe that the most non-trivial instances of phase separation, which are also those that can be triggered simply by density changes (e.g. by addition or removal

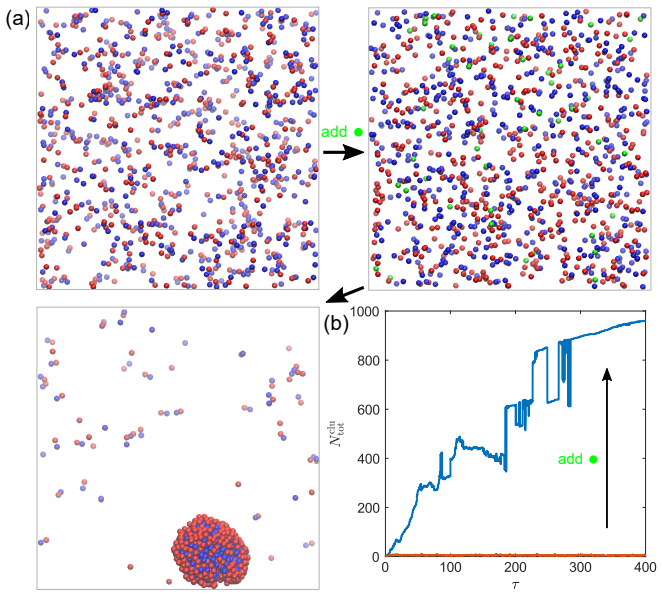

FIG. 3. Phase separation induced by a small amount of an active "doping agent". (a) Simulation snapshots showing macroscopic aggregation of a previously homogeneous mixture ($N_1 = N_2 = 500$, $\tilde{\alpha}_1 = \tilde{\mu}_1 = 1$, $\tilde{\alpha}_2 = -1$, $\tilde{\mu}_2 = 1/2$) after addition of 5 % of a third species ($N_3 = 50$, $\tilde{\alpha}_3 = -5$, $\tilde{\mu}_3 = 2$), compare movies 1 and 10 in the Supplemental Material [24]. (b) Time evolution of the size of the largest cluster (total number of particles), in the absence and presence of the third species.

of particles), occur in regions with such chasing interactions, which are in turn a direct signature of nonequilibrium activity.

Fourier analysis [24] of the simulation results (44 simulations with varying N_i, α_i, and μ_i; see Table S1 in the Supplemental Material [24]) agrees quantitatively with the theoretical prediction (2) for the stoichiometry at the onset of the instability; see Fig. 2(c). However, this initial value is not representative of the long-time stoichiometry of the phases. For $(\alpha_1, \alpha_2) = (+, +)$ mixtures, shown in Figs. 1(c) and 2(b), we always observe final configurations with either complete aggregation or separation of the two species. For $(\alpha_1, \alpha_2) = (+, -)$ mixtures, shown in Figs. 1(a) and 2(a), we always observe complete separation, but aggregation in this case leads to a cluster with non-trivial stoichiometry (Fig. 1(a), centre). Phenomenologically, we observe that the formation of such clusters proceeds by fast initial aggregation of the particles of the self-attractive species ($\alpha_i \mu_i < 0$) followed by slower recruitment of particles of the self-repelling species ($\alpha_i \mu_i > 0$) until the cluster is chemically "neutral", in the sense that its net consumption or production of chemicals vanishes, namely

$$\alpha_1 N_1^{\mathrm{clu}} + \alpha_2 N_2^{\mathrm{clu}} = 0, \tag{3}$$

where N_i^{clu} is the number of particles of species i in the cluster. The long-time stoichiometry of the clusters thus depends on the activity of the species, but it is independent of their mobility; see Fig. 2(d). An intuitive explanation for this observation can be provided as follows: once the cluster becomes neutral, the remaining self-repelling particles will no longer "sense" its presence and stay in a dilute phase. However, at high values of activity and mobility for the self-attractive species, deep inside the instability region, these static neutral clusters can become unstable *via* shape-symmetry breaking towards a self-propelled asymmetric cluster (Fig. 1(b)), which also involves the "shedding" of some of the self-repelling particles; see Fig. S3 and movies 8 and 9 in the Supplemental Material [24]. Finding a precise criterion for this symmetry-breaking to occur remains an open question, but we note that the manifestation of self-propulsion by the clusters is an intrinsically nonequilibrium feature.

Going beyond binary mixtures ($M > 2$), the phase separation phenomenology becomes even more complex due to the increasing number of parameter combinations, leading to a large variety of possible interaction networks between the different species. The instability condition (1) remains extremely useful, however. As a first example, in Fig. 3 we demonstrate how a small amount of a highly active "dopant" third species can be added to an otherwise homogeneous binary mixture in order to trigger macroscopic phase separation of the whole mixture on demand; see also movie 10 in the Supplemental Material [24]. As a second example, we have simulated highly polydisperse mixtures made up of 20 different species with activities and mobilities randomly chosen in the intervals $-2 \leq \tilde{\alpha}_i, \tilde{\mu}_i \leq +2$ for each species; see Fig. 1(d) and movies 11 and 12. We find that the instability criterion (1) can rather reliably distinguish between phase-separating and homogeneous mixtures; see Fig. S4 in the Supplemental Material [24]. We note that while all mixtures we predicted to phase-separate did so, some mixtures for which we predicted a linearly-stable homogeneous state were observed to phase-separate, albeit more slowly, once again pointing to a nucleation-and-growth mechanism rather than to a linear instability.

We have presented here a minimal model for phase separation in mixtures of chemically-interacting particles, and the generic phenomena that we predict should be applicable to a wide variety of systems. In the context of morphogenesis and collective migration in bacterial colonies and cells in tissues, the prediction of a transition between static and self-propelled clusters is particularly interesting. Here, it is important to take into account that what we call here "two species" may also represent a single species in two distinct states, each with different chemical activity or chemotactic behaviour. Regarding metabolon formation by enzymes in catalytic pathways, our prediction of "neutral" clusters (Eq. 3) is most intriguing, as it would correspond to a cluster in which

one enzyme channels all of its product to be taken as substrate by the next enzyme, with no substrate missing or in excess. Finally, our predictions can be tested in detail in experiments using synthetic catalytic colloids, by systematically varying the sign and magnitude of the chemical activity, as well as the concentration of the different species. In future work, it will be interesting to characterize in more detail the non-equilibrium activity of the system by means of its energy dissipation or entropy production [38, 39]. Moreover, we note that in our simulations we have neglected hydrodynamic interactions between particles as well as near-field contributions in the chemical concentrations [24]. While we we do not expect our results for the onset and stoichiometry of the instability to change, the detailed dynamics of aggregation and growth of the clusters as well as their internal dynamics will be affected by these additional effects.

This study was supported by the US National Science Foundation under MRSEC Grant number DMR-1420620.

* jaime.agudocanalejo@physics.ox.ac.uk
† ramin.golestanian@ds.mpg.de

[1] G. H. Wadhams and J. P. Armitage, Nat. Rev. Mol. Cell Biol. **5**, 1024 (2004).
[2] P. J. M. Van Haastert and P. N. Devreotes, Nat. Rev. Mol. Cell Biol. **5**, 626 (2004).
[3] S. Sengupta, K. K. Dey, H. S. Muddana, T. Tabouillot, M. E. Ibele, P. J. Butler, and A. Sen, J. Am. Chem. Soc. **135**, 1406 (2013).
[4] A.-Y. Jee, S. Dutta, Y.-K. Cho, T. Tlusty, and S. Granick, Proc. Natl. Acad. Sci. U. S. A. **115**, 14 (2018).
[5] J. Agudo-Canalejo, P. Illien, and R. Golestanian, Nano Lett. **18**, 2711 (2018).
[6] J. L. Anderson, Annu. Rev. Fluid Mech. **21**, 61 (1989).
[7] R. Soto and R. Golestanian, Phys. Rev. Lett. **112**, 068301 (2014).
[8] R. Soto and R. Golestanian, Phys. Rev. E **91**, 052304 (2015).
[9] R. Niu, T. Palberg, and T. Speck, Phys. Rev. Lett. **119**, 028001 (2017).
[10] R. Niu, A. Fischer, T. Palberg, and T. Speck, ACS Nano **12**, 1093210938 (2018).
[11] T. Yu, P. Chuphal, S. Thakur, S. Y. Reigh, D. P. Singh, and P. Fischer, Chem. Commun. **54**, 11933 (2018).
[12] A. Varma, T. D. Montenegro-Johnson, and S. Michelin, Soft Matter **14**, 7155 (2018).
[13] B. Rallabandi, F. Yang, and H. A. Stone, arXiv (2019), arXiv:1901.04311.
[14] L. Keller and M. G. Surette, Nat. Rev. Microbiol. **4**, 249 (2006).
[15] M. E. Hibbing, C. Fuqua, M. R. Parsek, and S. B. Peterson, Nat. Rev. Microbiol. **8**, 15 (2010).
[16] P. Friedl and D. Gilmour, Nat. Rev. Mol. Cell Biol. **10**, 445 (2009).
[17] L. J. Sweetlove and A. R. Fernie, Nat. Commun. **9**, 2136 (2018).
[18] F. Wu, L. N. Pelster, and S. D. Minteer, Chem. Commun. **51**, 1244 (2015).
[19] X. Zhao, H. Palacci, V. Yadav, M. M. Spiering, M. K. Gilson, P. J. Butler, H. Hess, S. J. Benkovic, and A. Sen, Nat. Chem. **10**, 311 (2018).
[20] T. Schwander, L. Schada von Borzyskowski, S. Burgener, N. S. Cortina, and T. J. Erb, Science **354**, 900 (2016).
[21] J. Palacci, S. Sacanna, A. P. Steinberg, D. J. Pine, and P. M. Chaikin, Science **339**, 936 (2013).
[22] H. Massana-Cid, J. Codina, I. Pagonabarraga, and P. Tierno, Proc. Natl. Acad. Sci. U. S. A. **115**, 10618 (2018).
[23] A. V. Ivlev, J. Bartnick, M. Heinen, C. R. Du, V. Nosenko, and H. Löwen, Phys. Rev. X **5**, 011035 (2015).
[24] See Supplemental Material at [URL will be inserted by publisher] for details on the linear stability analysis of the continuum model, the Brownian dynamics simulations, and the Fourier analysis of the initial stoichiometry; Supplemental Figures S1–S4 and Table S1; movies 1–12 and a description of the movies.
[25] T. Vicsek, A. Czirok, E. Ben-Jacob, I. Cohen, and O. Shochet, Phys. Rev. Lett. **75**, 1226 (1995).
[26] J. Toner and Y. Tu, Phys. Rev. E **58**, 4828 (1998).
[27] R. Golestanian, Phys. Rev. Lett. **108**, 038303 (2012).
[28] Y. Fily and M. C. Marchetti, Phys. Rev. Lett. **108**, 235702 (2012).
[29] G. S. Redner, M. F. Hagan, and A. Baskaran, Phys. Rev. Lett. **110**, 055701 (2013).
[30] S. Saha, R. Golestanian, and S. Ramaswamy, Phys. Rev. E **89**, 062316 (2014).
[31] J. A. Cohen and R. Golestanian, Phys. Rev. Lett. **112**, 068302 (2014).
[32] A. Zöttl and H. Stark, Phys. Rev. Lett. **112**, 118101 (2014).
[33] O. Pohl and H. Stark, Phys. Rev. Lett. **112**, 238303 (2014).
[34] M. E. Cates and J. Tailleur, Annu. Rev. Condens. Matter Phys. **6**, 219 (2015).
[35] B. Liebchen, D. Marenduzzo, I. Pagonabarraga, and M. E. Cates, Phys. Rev. Lett. **115**, 258301 (2015).
[36] B. Liebchen, D. Marenduzzo, and M. E. Cates, Phys. Rev. Lett. **118**, 268001 (2017).
[37] E. F. Keller and L. A. Segel, J. Theor. Biol. **26**, 399 (1970).
[38] B. Sabass and U. Seifert, J. Chem. Phys. **136**, 064508 (2012).
[39] P. Gaspard and R. Kapral, J. Chem. Phys. **148**, 134104 (2018).
[40] P. Strating, Phys. Rev. E **59**, 2175 (1999).
[41] A. Y. Toukmaji and J. A. Board, Comput. Phys. Commun. **95**, 73 (2003).